Probabilistic Engineering Mechanics 59 (2020) 103032

Contents lists available at ScienceDirect

Probabilistic Engineering Mechanics

journal homepage: www.elsevier.com/locate/probengmech

Probability density evolution analysis of stochastic seismic response of structures with dependent random parameters

Zhiqiang Wan, Jianbing Chen *, Jie Li

State Key Laboratory of Disaster Reduction in Civil Engineering & College of Civil Engineering, Tongji University, 1239 Siping Road, Shanghai 200092, PR China

ARTICLE INFO

Keywords:
Correlation
Dependent random parameters
Nonlinearity
Concrete structure
Probability density evolution method

ABSTRACT

Performance evaluation and reliability assessment of real-world structures under earthquakes is of paramount importance. Generally, different mechanical property parameters of a structure are usually not independent, nor completely dependent, but partly dependent or correlated. Therefore, how to reasonably characterize such partial dependency and whether such partial dependency real matters in the stochastic response and reliability of structures under earthquakes are crucial issues. For this purpose, in the present paper, a novel physically-guided data-driven methodology of capturing the correlation configuration of basic random variables and the probability density evolution method are synthesized. The physically-guided data-driven methodology is firstly outlined. In this methodology, the underlying physical mechanism between dependent random variables is firstly involved to establish a random function model, and then the available observed data are adopted to identify the parameters in this model. What is more, physical constraints are also revealed for the initial modulus of elasticity and compressive strength of concrete. The probability density evolution method is then adopted, and the point selection by minimizing the GF-discrepancy is adjusted according to the correlation configuration and physical constraints. A reinforced concrete frame structure subjected to earthquake input is studied. It is found that when the structure is in the strongly nonlinear stage, the correlation configuration has considerable effects on the standard deviation of the stochastic responses, by a factor of nearly 2. In addition, whether the mechanical parameters in different floors are independent or not has great effects on the stochastic responses as well. Problems to be further studied are also outlined.

1. Introduction

Reasonable quantification of mechanical properties of construction materials is crucial for the seismic performance evaluation and reliability analysis of structures. These mechanical properties are to be taken as random variables or random fields, and are usually correlated. For the sake of simplicity, however, in most practical applications, these random variables are either considered to be independent, or completely dependent. For instance, in the widely used orthogonal polynomial expansion method, the basic random variables are usually assumed to be independent [1–3]. In contrast, in engineering practice it is widely recommended that the initial modulus of elasticity of concrete is determined deterministically according to the compressive strength in an empirical relationship [4], which implies a perfect, though, nonlinear dependency between the two random variables. However, it was well recognized from experimental data that these two mechanical parameters of concrete are partly correlated in nature [5,6]. In static reliability of structures it has been demonstrated that such correlation has great effect on structural reliability assessment [7,8]. Then the following two questions arise: what is the reasonable probabilistic model that can capture such correlations? What is the effect of such correlation on the stochastic response and reliability of structures under earthquakes?

The methodology of capturing partially correlation between two random variables based on data can be broadly classified into two types: one is to find an appropriate joint probability density function (PDF) by hypothesis and test; and the other is to find a random function relationship between the two random variables so that the dependent random variables can be converted into independent random variables. To the former class belonging, for instance, the copula function has been applied in soil and rock engineering [9,10] to find a joint PDF with known marginal PDFs and a deterministic copula function. Nevertheless, the selection of form of copula function is usually difficult and somewhat empirically based. On the other hand, to the second type belonging, e.g., the Rosenblatt transformation [11] and the polynomial chaos expansion [12], are widely employed in practice, where the dependency is represented by strong nonlinear transforms. Though converting dependent random variables to independent basic random variables, unfortunately such transforms will usually worsen, more or

* Corresponding author.
E-mail addresses: wanzhiqiang@tongji.edu.cn (Z. Wan), chenjb@tongji.edu.cn (J. Chen), lijie@tongji.edu.cn (J. Li).

https://doi.org/10.1016/j.probengmech.2020.103032
Received 17 January 2020; Accepted 29 January 2020
Available online 1 February 2020

less, the well-posedness of the problem in many cases. For instance, due to such transformations, the accuracy of point estimate of moments of response may be considerably deteriorated [13].

Recently, based on the thought of physically-guided data-driven (PGDD) modeling methodology, Chen et al. [6] proposed a new random function model, which is of weak nonlinearity, to capture the correlation configuration of dependent random variables. Based on this random function model, the correlation between the modulus of elasticity E_c and the compressive strength f_c of concrete was investigated. Remarkably, in this random function model the underlying physical background was advocated, and therefore, two physical constraints, as byproducts of modeling, were also obtained. These two physical constraints will guide and adjust the point selection, which is an important step in the probability density evolution method (PDEM, [14]). In this paper, the stochastic responses of a reinforced concrete (RC) frame structure subjected to earthquake acceleration are analyzed. The cases with completely independent (CI) basic random vector, completely dependent (CD) basic random vector [4], and partially dependent (PD) basic random vector [6] are studied and compared. The results indicate that the effect of correlation configuration of mechanical properties is unignorable for the stochastic response of structures.

2. Representation of dependent random variables

2.1. Random function model for dependent random variables

For clarity, considering two dependent random variables X and Y. In Chen et al. [6], the dependency between X and Y is written as the following form of random function

$$Y = g_1(X) + \zeta \cdot g_2(X) \tag{1}$$

where ζ is a random variable with zero mean and unity variance, and is independent to X. The two weak nonlinear functions $g_1(\cdot)$ and $g_2(\cdot)$ are to be determined, either by physical reasoning or data learning. Further, by conducting the conditional expectation on both sides of Eq. (1), we have

$$\mathbb{E}[Y|X] = g_1(X) \tag{2}$$

where $\mathbb{E}[\cdot]$ denotes the expectation operator. This means that $g_1(\cdot)$ is nothing but the conditional mean function, which is the optimal function satisfying the minimum mean squared error (MSE) as well [15]. Similarly, the conditional variance function can be deduced as

$$\mathbb{E}\left[(Y - \mathbb{E}[Y|X])^2 |X\right] = g_2^2(X), \tag{3}$$

which means that the function $g_2(\cdot)$ is actually the conditional standard deviation function.

Hence, the dependent random vector (X, Y) can be converted into an independent random vector (X, ζ) by the random function (1). Generally, the conditional mean function and the conditional standard deviation function are nonlinear functions, but the nonlinearity is usually weak. In fact, Eqs. (2) and (3) are closely associated with specific physical backgrounds, e.g., the conditional mean function captures the major tendency of Y with respect to X, whereas the conditional standard deviation function represents the degree of uncertainty of Y in terms of X, respectively. As mentioned, the functions $g_1(\cdot)$ and $g_2(\cdot)$ are to be determined by the embedded physical mechanism, or simply inferred statistically. The probability distribution of the auxiliary variable ζ can be also determined either by the embedded physical mechanism, or more frequently be determined by statistical inference of observed data. In the latter case, the ith sample value of ζ is calculated by

$$\zeta_i = \frac{y_i - g_1(x_i)}{g_2(x_i)} \tag{4}$$

where (x_i, y_i) is the ith sample point of the random vector (X, Y).

2.2. Physically-guided data-driven (PGDD) methodology

To determine the functions $g_1(\cdot)$ and $g_2(\cdot)$, a physically-guided data-driven (PGDD) methodology was proposed [6], where the compressive strength of concrete f_c and the initial modulus of elasticity of concrete E_c are taken into investigation. To this end, the shape of the two basic functions are determined by advocating the underlying physical mechanism of concrete materials. For instance, in Refs. [16] and [17], a simple rheological model was proposed to describe the mechanical behavior of concrete subjected to uniaxial compression. This model consists of two parts: the Hooke part representing the elasticity of concrete and the Kelvin part reflecting the viscoelasticity of concrete, respectively. It was then derived, by taking the secant modulus as the modulus of elasticity, where $\sigma = \beta f_c$, such that [16]

$$\frac{1}{E_c} = \frac{E_1 + E_2}{E_1 E_2} - \frac{K\upsilon}{E_2^2 \beta}\frac{1}{f_c}\left(1 - \exp\left(-\frac{\beta E_2}{\upsilon K} f_c\right)\right), \tag{5}$$

where E_1, E_2, K and υ are parameters of the rheological model as shown in [16]. Rewriting Eq. (5), after taking $A = \frac{E_1+E_2}{E_1 E_2}$, $B = -\frac{K\upsilon}{E_2^2\beta}$, $C = \frac{\beta E_2}{\upsilon K}$, leads to

$$\frac{1}{E_c} = A + B\frac{1}{f_c}\left(1 - \exp\left(-C f_c\right)\right) \tag{6}$$

where A, B and C are constants. Till now, a clear relation is generated between E_c and f_c.

2.2.1. Conditional mean function

For engineering purposes, concise but meaningful expression is needed. When $\exp(-C f_c) \to 0$, Eq. (6) can be simplified into

$$\frac{1}{E_c} \approx A + B\frac{1}{f_c}. \tag{7}$$

It reveals that the reciprocal of modulus of elasticity is in linear relationship with the reciprocal of compressive strength of concrete [6,16], which is actually adopted by Chinese code for design of concrete structures [4].

Since Eq. (7) can reflect the major relation between E_c and f_c, the form of $g_1(\cdot)$ can be determined accordingly as

$$g_1(f_c) = \frac{1}{a_1 + b_1 \frac{1}{f_c}} \tag{8}$$

where a_1 and b_1 should be identified from experimental data by Eq. (2), see [6] for the details. Here, the lower-case letters a_1 and b_1 are utilized for identified deterministic parameters, corresponding to the former parameters A and B in Eq. (7), respectively.

2.2.2. Conditional standard deviation function

By Eq. (3), it is noticed that the conditional standard deviation function is based on the difference between the conditional mean function and the dependent variable, Y (i.e., E_c). Hence, by taking the absolute value of the residual as $|\Delta| = \left|E_c - g_1(f_c)\right|$, according to Eq. (3) there is

$$g_2(f_c) = \sqrt{\mathbb{E}\left[|\Delta|^2\right]} = \mathcal{O}(\mathbb{E}[|\Delta|]) \tag{9}$$

where $\mathcal{O}(\cdot)$ denotes the quantity of the same order of magnitude.

Further, substituting Eqs. (6) and (7) in it leads to

$$|\Delta| = \left|E_c - \frac{1}{A + B\frac{1}{f_c}}\right| \approx \frac{B f_c}{(A + B f_c)^2} \cdot \exp(-C f_c) = \mathcal{O}(\mathbb{E}[|\Delta|]). \tag{10}$$

The second equality in Eq. (10) means that, by statistical inference of $|\Delta|$ and f_c, we can have an optimal estimation of $|\Delta|$ with the minimum mean squared error, which is a proper form of $g_2(f_c)$ as well. Therefore, we have

$$g_2(f_c) = \frac{b_2 f_c}{(a_2 + b_2 f_c)^2} \cdot \exp(-c f_c) \tag{11}$$

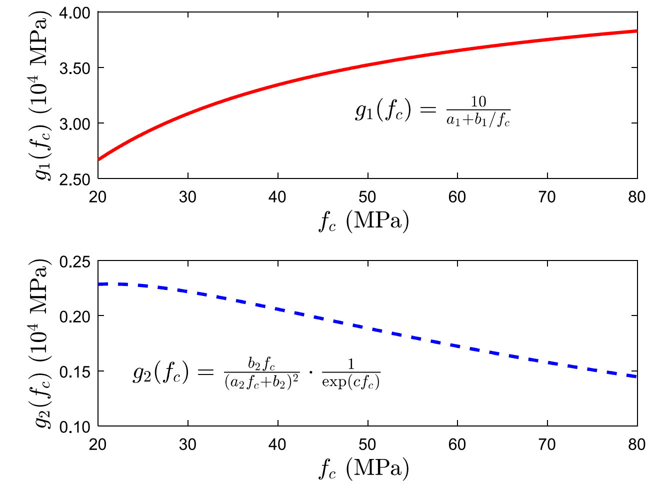

Fig. 1. The random function model for the modulus of elasticity and compressive strength of concrete.

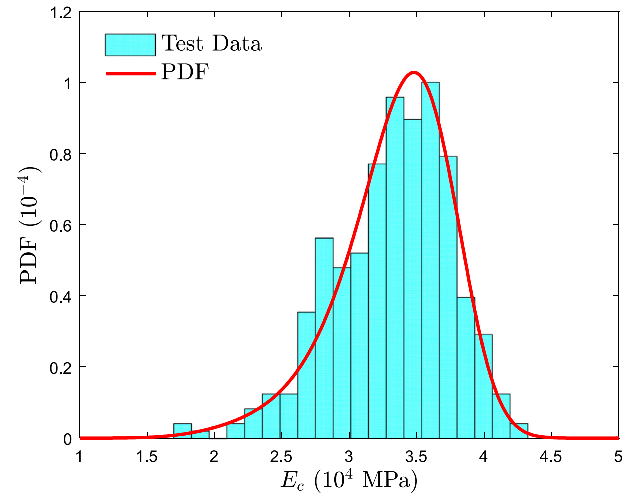

Fig. 2. The marginal PDF of E_c calculated by Eqs. (14) and (15) compared with the test data from [18] in the form of histogram.

where a_2, b_2 and c should be identified from the test data of $|\Delta|$ and f_c. With Eqs. (8) and (11) at hand, and by Eq. (4), the probability distribution of ζ can then be determined. It should be emphasized that to some degree of statistical errors, ζ may not be exactly but close to zero mean value and unity standard deviation. Actually, according to the data the mean value μ_ζ is 0.118 while the standard deviation σ_ζ is 1.38 [6]. Therefore, the random function finally takes

$$E_c = \frac{10}{a_1 + b_1/f_c} + (\zeta\sigma_\zeta + \mu_\zeta)\frac{b_2 f_c}{(a_2 f_c + b_2)^2} \cdot \frac{1}{\exp(c f_c)} \tag{12}$$

where all the undetermined parameters are specified in [6], taking the same procedure from Eqs. (5) to (11). Note that in Eq. (12) though the function looks complex, it is actually only weakly nonlinear in terms of f_c, and linear in terms of ζ, which can be seen clearly from Fig. 1.

Note that in the above modeling procedure the shape of the two functions are determined by physical reasoning, whereas the distribution of the auxiliary random variables and the parameters are identified from observed data. Such methodology of capturing the dependency between different random variables can be referred to as the physically-guided data-driven (PGDD) method.

Remark 1. Alternatively, when the random function model in Eq. (12) is established, the joint PDF of (f_c, E_c) can be derived easily by combining marginal PDFs of f_c and ζ and by the rule of change of random variable(s) [6]:

$$p_{f_c,E_c}(f_c, E_c) = \frac{1}{|g_2(f_c)|} p_{f_c}(f_c)\, p_\zeta\left(\zeta = \frac{E_c - g_1(f_c)}{g_2(f_c)}\right) \tag{13}$$

where the marginal PDF of f_c, i.e., $p_{f_c}(f_c)$, can be identified from test data [18] in the form of normal distribution with mean value $\mu_{f_c} = 41.81$ and standard deviation $\sigma_{f_c} = 14.14$;, the marginal PDF of ζ, i.e., $p_\zeta(\zeta)$, is determined by statistical inference from Eq. (4) and found to be normally distributed as well. Then the joint PDF $p_{f_c,E_c}(f_c, E_c)$ is derived as

$$\begin{cases} p_{f_c,E_c}(f_c, E_c) = \dfrac{(a_2 f_c + b_2)^2}{b_2 \sigma_\zeta f_c} \exp(c f_c) \times \dfrac{1}{2\pi\sigma_{f_c}} \exp\left\{-\dfrac{\sigma_{f_c}^2 \zeta^2 + (f_c - \mu_{f_c})^2}{2\sigma_{f_c}^2}\right\}, \\ \zeta = \dfrac{E_c - \frac{1}{a_1 + b_1/f_c} - \frac{\mu_\zeta b_2 f_c}{(a_2 f_c + b_2)^2 \exp(c f_c)}}{\sigma_\zeta b_2 f_c} \times (a_2 f_c + b_2)^2 \exp(c f_c) \end{cases} \tag{14}$$

Further, the marginal PDF of E_c can be easily derived by

$$p_{E_c}(E_c) = \int p_{f_c,E_c}(f_c, E_c)\, df_c. \tag{15}$$

The marginal PDF of E_c is drawn along with the test data in Fig. 2, and a good fitness is achieved. Notice that E_c is neither normally distributed by observations of the analytical PDF nor the histogram of test data.

2.2.3. Comparison of partial dependency and complete dependency

In the remaining parts, the unit of E_c takes 10^4 MPa while the unit of f_c takes MPa, respectively. Compared to the empirical relation in Chinese code for design of concrete structures [4,6]

$$E_c = \frac{10}{2.2 + \frac{34.7}{f_c}}. \tag{16}$$

It is seen clearly that the mean of Eq. (12) is almost identical to Eq. (16), but in Eq. (12) the fluctuating part is also involved.

2.3. Physical constraints and point set adjustment

2.3.1. Physical constraints for dependent mechanical parameters

Concrete, as a type of complex composite material, is remarkably featured by the randomness and nonlinearity in its mechanical behaviors. The former characteristic is due to the uncertainty of its mixture and micro-mechanical constitution, while the latter is due to its damage evolution when subjected to external loadings [19]. Clearly, the ascent stage of concrete subjected to uniaxial compression should satisfy Drucker's postulate [20], namely

$$d\sigma d\varepsilon^p \geqslant 0 \tag{17}$$

where $d\sigma$ is an incremental stress and $d\varepsilon^p$ denotes an increment of plastic strain. In short, the yielding surface of stable materials, e.g., concrete in its ascent stage, must be convex. Furthermore, for uniaxial compression, the following inequation holds

$$E_c > E_{sec} \tag{18}$$

where E_{sec} is the secant modulus of elasticity. By adopting more empirically physical relations [4,6], from Eq. (18) there is

$$\begin{cases} E_c > 0.83 f_c^{0.31} \\ E_c > 100 f_c \big/ \left(700 + 172\sqrt{f_c}\right) \end{cases}, \tag{19}$$

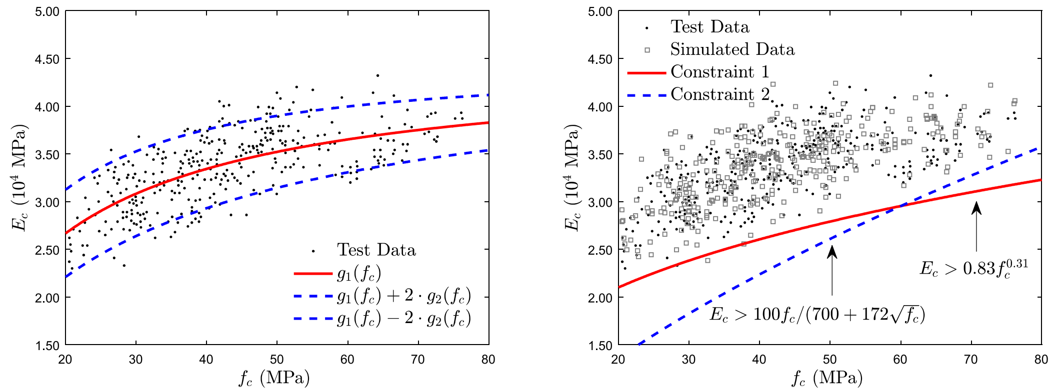

(a) The random function model and test data (b) The physical constraints and simulated data

Fig. 3. The random function model, physical constraints, test data and simulated data.

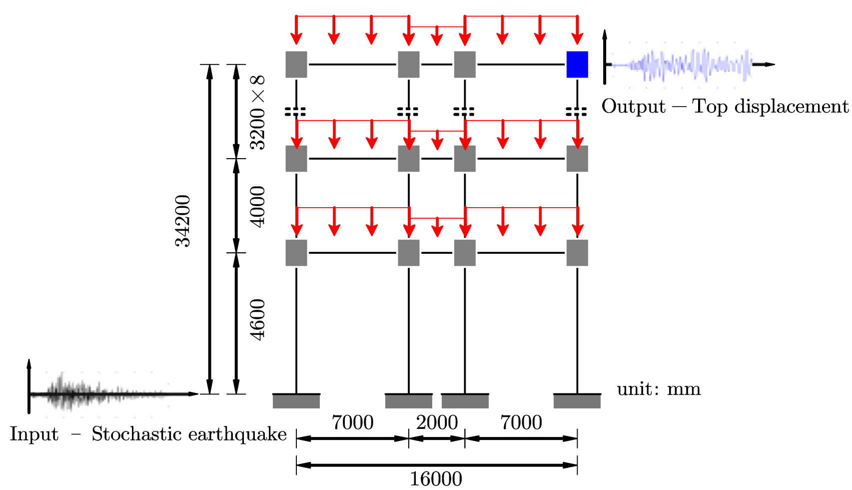

Fig. 4. Structural information.

which implies that E_c is not only dependent on f_c but also admits the underlying physical principles that satisfying Inequality (19). Therefore, the above two physically based constraints are imposed in the following analysis.

The random function model and the test data are displayed in Fig. 3(a). The test data are adapted from [18]. It can be seen that most of the data are in the range of $g_1(f_c) \pm 2 \cdot g_2(f_c)$, while $g_2(f_c)$ and $g_1(f_c)$ are weakly nonlinear in terms of f_c, as also illustrated in Fig. 1. This demonstrates that the random function model can capture the correlation between the two variables. The two physical constraints are plotted in Fig. 3(b), where both the test data and simulated data generated from the random function model are also shown. It is found remarkably that all the test data are above the two physical constraints, which verifies Inequality (19). However, there is one simulated point that is below the constraint, which is spurious due to the unbounded Gaussian distribution of ζ. There might be more spurious points if one repeats the simulation or increases the size of simulated data. In the crude Monte Carlo simulation, these spurious point samples can be simply abandoned since they are randomly generated. Nevertheless, in the PDEM analysis, the point set is generated by certain optimal strategies, e.g., the GF-discrepancy minimized strategy [21]. Therefore, the spurious samples cannot be directly discarded. Consequently, the adjustment of point set with certain physical constraints is needed, and will be discussed in Section 3.3 in details.

From the above, the PGDD is featured by: (i) the form of the basic functions is determined by the underlying physical mechanism, which makes the model more objective than the phenomenologically fitted ones because usually different inference or fitting methods, either parametric or non-parametric, may lead to different results; (ii) the correlation between the random variables is captured by two weakly nonlinear functions that will not worsen the well-posedness of the problem; and (iii) during the modeling procedure, more valuable information, e.g., some inherent physical principles may be revealed. It is noted that the PGDD is essentially consistent with the thought of physical modeling of stochastic excitations [22,23].

3. Fundamentals of PDEM and point selection strategy

3.1. Fundamentals of PDEM

For clarity, we start with an outline of the probability density evolution method [14]. Without loss of generality, consider a stochastic dynamical system

$$\dot{\mathbf{X}} = \mathcal{G}(\mathbf{X}, \mathbf{\Theta}, t) \tag{20}$$

where $\mathbf{X}=(X_1,\ldots,X_m)^{\mathrm{T}}$ is an m-dimensional state vector with the initial condition $\mathbf{X}(t_0) = \mathbf{X}_0$, $\mathcal{G}(\cdot)$ denotes a state mapping and $\mathbf{\Theta} = (\Theta_1,\ldots,\Theta_s)^{\mathrm{T}}$ is an s-dimensional random vector with the joint PDF $p_{\mathbf{\Theta}}(\boldsymbol{\theta})$. For well-posed problems, the solution of Eq. (20) can be denoted by $\mathbf{X} = \mathcal{H}(\mathbf{X}_0, \mathbf{\Theta}, t)$ with its components $X_\ell = \mathcal{H}_\ell(\mathbf{X}_0, \mathbf{\Theta}, t)$ for $\ell = 1,\ldots,m$. The generalized velocity can be denoted as $\dot{\mathbf{X}} = h(\mathbf{X}_0, \mathbf{\Theta}, t)$ with its components $\dot{X}_\ell = h_\ell(\mathbf{X}_0, \mathbf{\Theta}, t)$ for $\ell = 1,\ldots,m$, respectively.

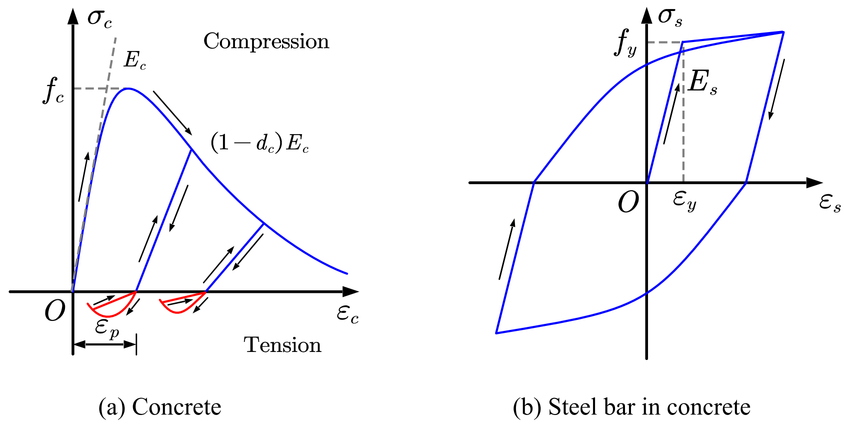

Fig. 5. Constitutive models of concrete and steel bars.

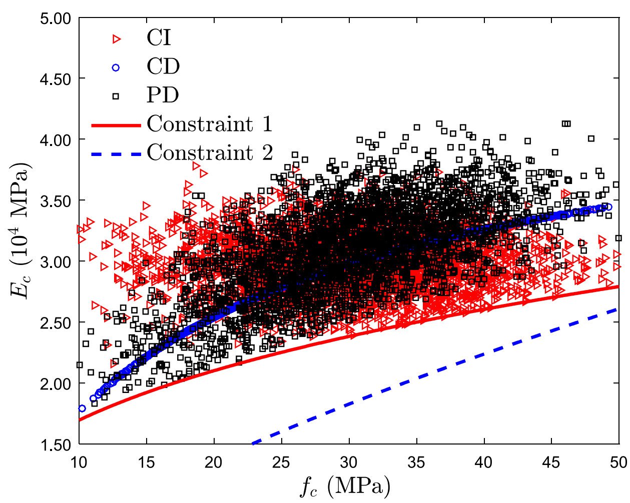

Fig. 6. Adjusted point sets corresponding to three different correlation configurations.

According to the principle of preservation of probability [24], the joint PDF of $(\mathbf{X}(t), \boldsymbol{\Theta})$, denoted by $p_{\mathbf{X}\boldsymbol{\Theta}}(\mathbf{x}, \boldsymbol{\theta}, t)$, is governed by

$$\frac{\partial p_{\mathbf{X}\boldsymbol{\Theta}}(\mathbf{x}, \boldsymbol{\theta}, t)}{\partial t} + \sum_{\ell=1}^{m} \dot{X}_{\ell}(\boldsymbol{\theta}, t) \frac{\partial p_{\mathbf{X}\boldsymbol{\Theta}}(\mathbf{x}, \boldsymbol{\theta}, t)}{\partial x_{\ell}} = 0, \tag{21}$$

which is called the generalized density evolution equation (GDEE). More generally, when we focus on only one quantity of interest (QoI), e.g., the ℓth component X (the subscript ℓ is omitted in the following part without inducing confusion), then Eq. (21) is reduced to

$$\frac{\partial p_{X\boldsymbol{\Theta}}(x, \boldsymbol{\theta}, t)}{\partial t} + \dot{X}(\boldsymbol{\theta}, t) \frac{\partial p_{X\boldsymbol{\Theta}}(x, \boldsymbol{\theta}, t)}{\partial x} = 0. \tag{22}$$

By solving Eq. (22) and integrating in terms of $\boldsymbol{\Theta}$, one immediately has

$$p_X(x, t) = \int_{\Omega_{\boldsymbol{\Theta}}} p_{X\boldsymbol{\Theta}}(x, \boldsymbol{\theta}, t)\, \mathrm{d}\boldsymbol{\theta} \tag{23}$$

where $p_X(x, t)$ is the PDF of QoI and $\Omega_{\boldsymbol{\Theta}}$ is the distribution domain of $\boldsymbol{\Theta}$.

In general, the numerical procedure for solving GDEE involves four steps [14]:

Step 1.1: Partition of random parameter space $\Omega_{\boldsymbol{\Theta}}$ with a certain point selection strategy [25]. Suppose the domain $\Omega_{\boldsymbol{\Theta}}$ is partitioned into n_{sel} domains, and in each domain one representative point $\boldsymbol{\theta}_q$ is specified. In short, a point set denoted by $\mathcal{M} = \{\boldsymbol{\theta}_q\}_{q=1}^{n_{\mathrm{sel}}}$ is generated in this step by a certain point selection strategy. More details are illustrated in Section 3.2.

Step 1.2: Deterministic analysis with the representative points. For each representative point $\boldsymbol{\theta}_q$, the deterministic analysis is conducted for Eq. (20) by setting $\boldsymbol{\Theta} = \boldsymbol{\theta}_q$, and the corresponding QoI, i.e., $\dot{X}(\boldsymbol{\theta}_q, t)$, is obtained.

Step 1.3: Solving GDEE. For each representative point $\boldsymbol{\theta}_q$ with corresponding $\dot{X}(\boldsymbol{\theta}_q, t)$ from Step 1.2, solve the partially discretized version of Eq. (22)

$$\frac{\partial p^{(q)}_{X\boldsymbol{\Theta}}(x, \boldsymbol{\theta}_q, t)}{\partial t} + \dot{X}(\boldsymbol{\theta}_q, t) \frac{\partial p^{(q)}_{X\boldsymbol{\Theta}}(x, \boldsymbol{\theta}_q, t)}{\partial x} = 0, \quad q = 1, \ldots, n_{\mathrm{sel}}. \tag{24}$$

Step 1.4: Synthesizing the results from Step 1.3. The PDF of QoI is finally obtained by

$$p_X(x, t) = \sum_{q=1}^{n_{\mathrm{sel}}} p^{(q)}_{X\boldsymbol{\Theta}}(x, \boldsymbol{\theta}_q, t). \tag{25}$$

It should be emphasized that there is no assumption of independency of basic random variables in PDEM theoretically.

3.2. Point selection strategy in PDEM

For clarity and completeness, the point selection strategy of PDEM in Step 1.1 will be detailed herein. In the point selection strategy by minimizing the GF-discrepancy [21,26], there are three major steps:

Step 2.1: Generate an initial point set $\mathcal{M}^{(0)} = \{\boldsymbol{\theta}_q\}_{q=1}^{n_{\mathrm{sel}}}$. Denote the n_{sel} initial points by $\boldsymbol{\theta}_q = (\theta_{q,1}, \ldots, \theta_{q,s})^{\mathrm{T}}$, $q = 1, \ldots, n_{\mathrm{sel}}$, where s is the dimension of the vector $\boldsymbol{\theta}_q$. For instance, the Sobol' sequence is suggested to generate this initial point set, but any other low-discrepancy point set is also feasible.

Step 2.2: Point set rearrangement – the first round. Convert the initial point set by

$$\theta'_{k,i} = F_i^{-1}\left(\sum_{q=1}^{n_{\mathrm{sel}}} \frac{1}{n_{\mathrm{sel}}} \cdot I\{\theta_{q,i} < \theta_{k,i}\} + \frac{1}{2} \cdot \frac{1}{n_{\mathrm{sel}}}\right) \text{for } i = 1, \ldots, s,\ k = 1, \ldots, n_{\mathrm{sel}} \tag{26}$$

where $F_i^{-1}(\cdot)$ is the inverse of cumulative distribution function (CDF) of the ith dimension, and $I\{\cdot\}$ is an indicator function with value being one if the bracket event is true and otherwise zero. By doing so, a new point set $\mathcal{M}^{(1)} = \{\boldsymbol{\theta}'_q\}_{q=1}^{n}$ is generated with a relative low discrepancy.

Step 2.3: Point set rearrangement – the second round. To obtain a low GF-discrepancy, an additional rearrangement is required. First, the assigned probability for each point is specified by

$$P_q = \int_{V_q} p_{\boldsymbol{\Theta}}(\boldsymbol{\theta})\, \mathrm{d}\boldsymbol{\theta}, \quad q = 1, \ldots, n_{\mathrm{sel}} \tag{27}$$

where $p_{\boldsymbol{\Theta}}$ is the joint PDF of random vector $\boldsymbol{\Theta}$ and V_q is the qth partitioned sub-domain, which can take the Voronoi cell as elaborated

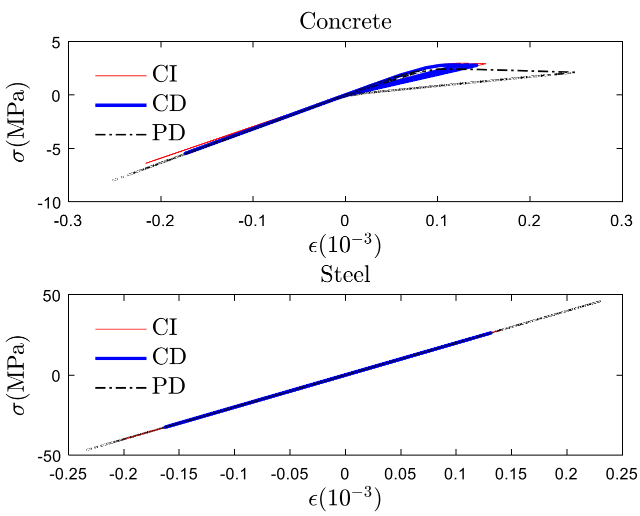

(a) Case 1: the PGA is set to 0.1g and the materials are almost linear

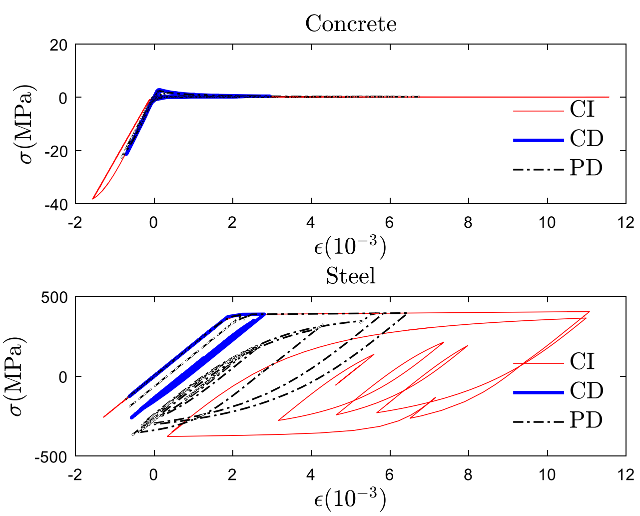

(b) Case 2: the PGA is set to 0.8g and the materials are of most nonlinearity

Fig. 7. Stress–strain curves of steel and concrete materials of case 1 and 2.

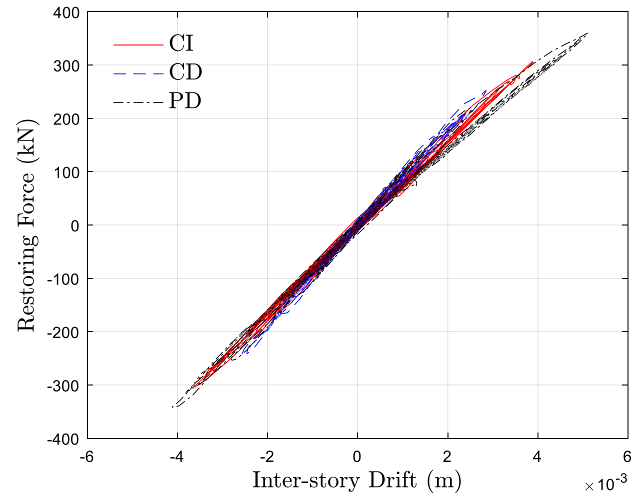

(a) Case 1: the PGA is set to 0.1g and the structure is almost at linear state

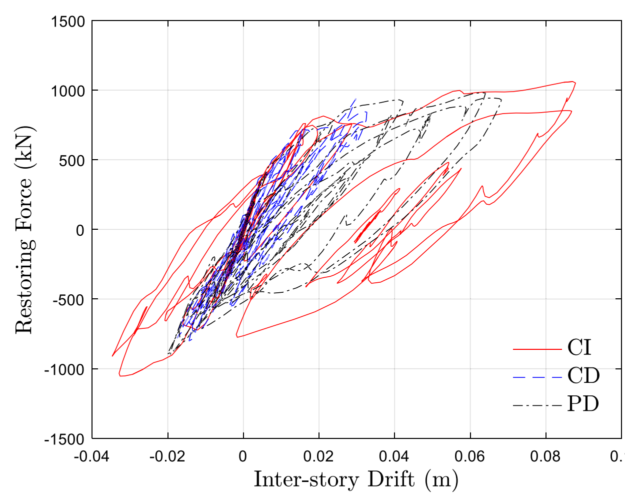

(b) Case 2: the PGA is set to 0.8g and the structure is almost of nonlinearity

Fig. 8. Typical hysteretic curve of restoring force vs. inter-story drift of case 1 and 2.

in Chen et al. [21]. By replacing the equal weight in Eq. (26), a second rearrangement can be written as

$$\theta''_{k,i} = F_i^{-1}\left(\sum_{q=1}^{n_{\mathrm{sel}}} P_q \cdot I\left\{\theta'_{q,i} < \theta'_{k,i}\right\} + \frac{1}{2}\cdot P_k\right) \text{ for } i = 1,\ldots,s,\ k = 1,\ldots,n_{\mathrm{sel}}. \tag{28}$$

Therefore, the final point set $\mathcal{M}^{(2)} = \left\{\theta''_q\right\}_{q=1}^{n_{\mathrm{sel}}}$ is generated with a low GF-discrepancy.

3.3. Point set adjustment in terms of physical constraints

As mentioned above, in reality, there exists some physical constraints for dependent mechanical parameters. Therefore, the point selection strategy in Section 3.2 should satisfy the underlying physical constrains. Thus, the following steps are taken.

Step 2.4: Point adjustment in terms of underlying physical constraints. The point set $\mathcal{M}^{(2)} = \left\{\theta''_q\right\}_{q=1}^{n_{\mathrm{sel}}}$ is sieved according to certain physical constraints, i.e., by Eq. (19). Denote the remaining point set as $\mathcal{M}^{(2),r} = \left\{\theta''_q\right\}_{q=1}^{n_r}$. Notice that this point set may have a relatively high GF-discrepancy compared to $\mathcal{M}^{(2)}$, thus another loop by Eq. (28) is needed. After several loops between Steps 2.3 and 2.4, a final point set denoted as $\mathcal{M}^{\mathrm{F}}$ is yielded. The GF-discrepancy of point set is thus minimized and all the representative points satisfy the certain physical constraints.

Remark 2. Notice that the above procedure of point selection strategy is utilized for independent random variables, e.g., (f_c, ζ). Then, we transform (f_c, ζ) into (f_c, E_c) by Eq. (12), of which f_c and E_c are naturally dependent. Since $g_1(\cdot)$ and $g_2(\cdot)$ are weakly nonlinear (as shown in Fig. 1), such a transformation will not considerably increase the point discrepancy of (f_c, E_c).

4. Numerical applications

4.1. Structural information

Consider a 10-story reinforced concrete frame structure as shown in Fig. 4. The external excitation is generated by a physical stochastic

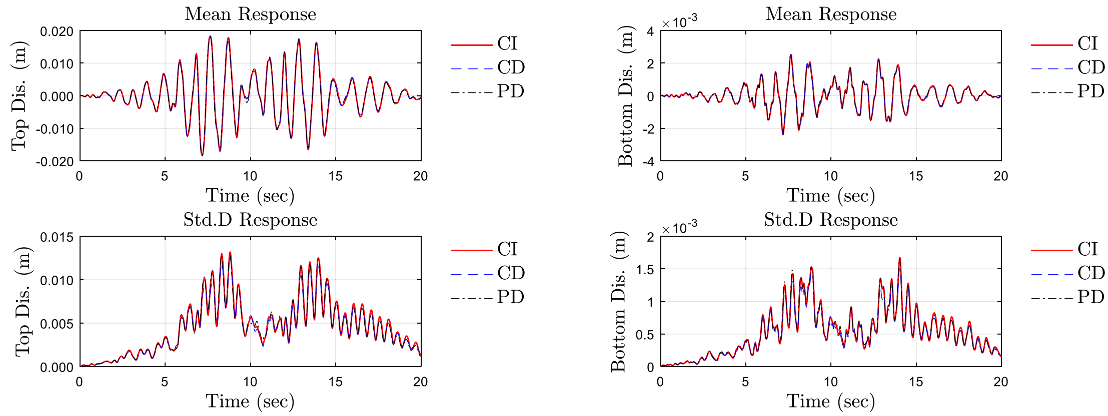

(a) Mean and Std.D displacement response of top and bottom in case 1 (0.1g)

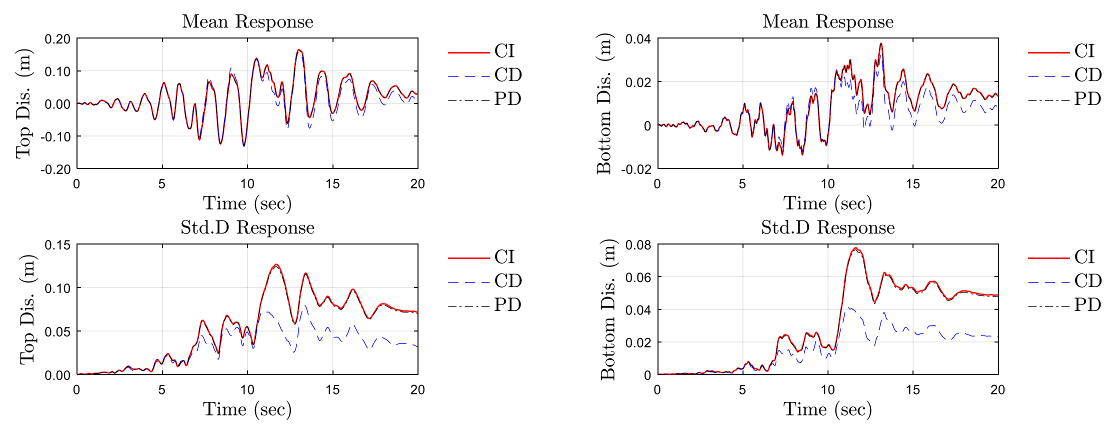

(b) Mean and Std.D displacement response of top and bottom in case 2 (0.8g)

Fig. 9. Statistics of structural displacement responses (each floor is independent).

model for earthquake ground motion process [27], which is physically based on the seismic source-path-site physical mechanism. The basic parameters of this model are A_0, τ, ξ_g and ω_g, with respect to the amplitude, the Brune source factor, the equivalent damping ratio and the equivalent predominant circular frequency, respectively. For more details, see [27] for the basic theories and [28] for engineering applications. The constitutive model of concrete in Chinese code for design of concrete structures [1,29] is adopted, while the constitutive model of steel is adopted from Filippou et al. [30]. The two constitutive models are available in OpenSEES software, corresponding to "ConcreteD" and "Steel02" commands, respectively. The stress–strain relations of the two materials are shown in Fig. 5.

Table 1
Model parameters with randomness (each story is independent).

Correlation	Parameters	Mean	Std.D	Distribution	Note
CI	$f_c^{(i)}$	30 MPa	6 MPa	Normal	–
	$E_c^{(i)}$	2.98×10^4 MPa	2.38×10^3 MPa	Normal	
CD	$f_c^{(i)}$	30 MPa	6 MPa	Normal	Eq. (16)
	$E_c^{(i)}$	–	–	–	
PD	$f_c^{(i)}$	30 MPa	6 MPa	Normal	Eq. (12)
	$\zeta^{(i)}$	0	1	Normal	
	$E_c^{(i)}$	–	–	–	

Annotation: $i = 1,\dots,10$ represents the story number from the 1st floor to the 10th floor, "Std.D" denotes the standard deviation, "CI" means complete independency, "CD" means complete dependency, "PD" means partial dependency.

The compressive strength f_c and the modulus of elasticity of concrete E_c are considered to be random variables. For the sake of simplicity, the mechanical parameters of columns and beams in the same story are assumed to be identical, while those in all 10 stories are mutually independent (Section 4.3) or completely dependent (Section 4.4). Details are available in Table 1. To investigate the influence of correlations between mechanical parameters, two cases are considered, denoted as Case 1 and Case 2. For Case 1, the peak ground acceleration (PGA) is modified to 0.1g, aiming to ensure the structure subjected to earthquake response in the linear stage; while for case 2, PGA is set to 0.8g, thus the structure is supposed to response in strongly nonlinear stage.

4.2. Probability density evolution analysis involving point set adjustment

As mentioned above, due to the underlying physical mechanisms, it is crucial to make an adjustment of the point set. The representative points for complete independency (CI), complete dependency (CD) and partial dependency (PD) are illustrated in Fig. 6. Some interesting properties are observed from these point sets: (1) all these points satisfy the physical constraints; (2) most of the points are gathered in the range of 24 MPa to 36 MPa in strength, which is an interval of mean ± standard deviation, i.e., 30 ± 6 MPa; and (3) for the points in the range of tail distribution (lower than 24 MPa or higher than 36 MPa in

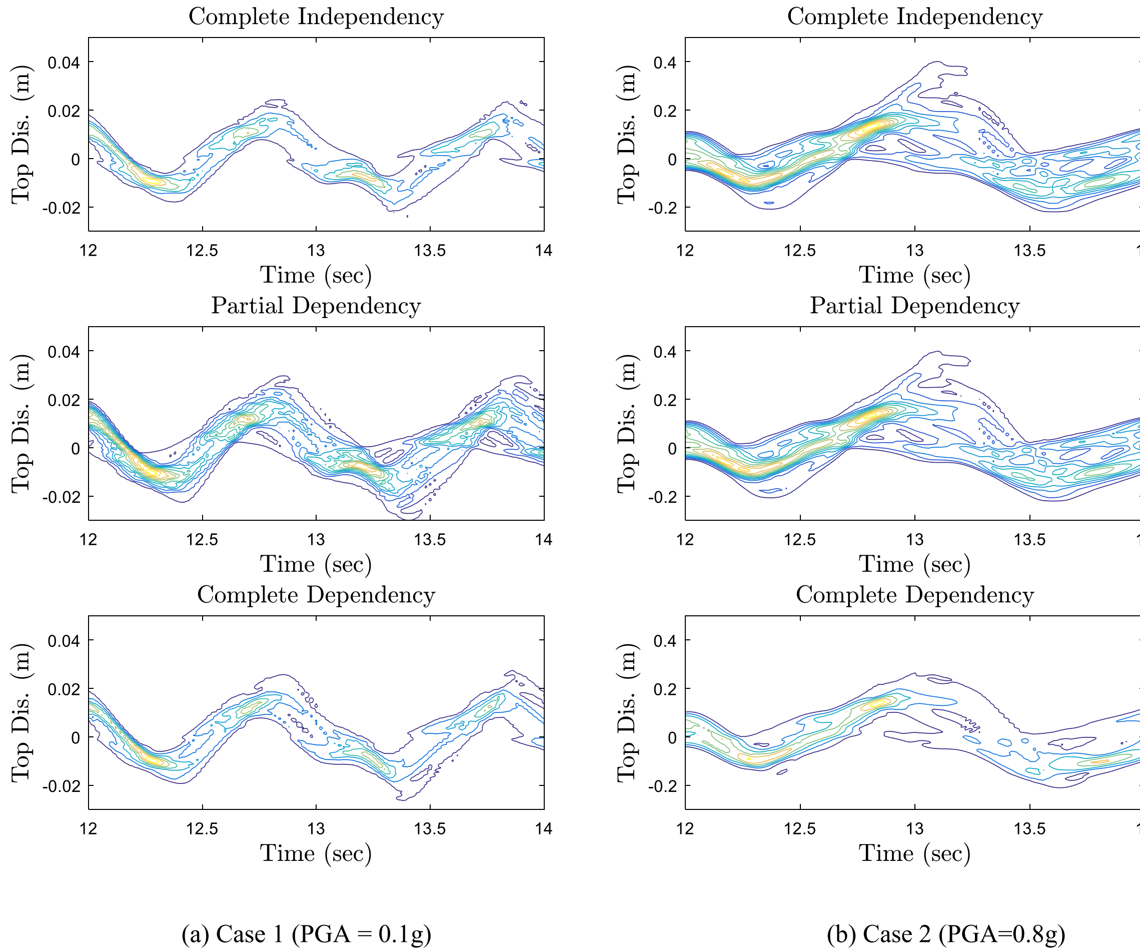

Fig. 10. Contours of PDFs for three correlation configurations.

strength), the modulus of elasticity in the points of CI and PD are quite different. We will see later that this property will lead to a closeness for the statistical moments but has remarkable influence on tails of PDF of QoI.

4.3. Stochastic responses of the structure involving material parameters with three correlation configurations

In this section, the mechanical properties of different stories are considered to be mutually independent, whereas in each story, three correlation configurations (CI, CD and PD) between the modulus of elasticity and compressive strength of concrete are considered for comparison.

4.3.1. Comparison between statistical moments of stochastic responses for different correlation configurations

The PDEM is adopted to carry out stochastic response analysis of the structure subjected to earthquake excitations. The typical samples of constitutive curves and of restoring force v.s. displacement are plotted in Figs. 7 and 8, respectively. It is observed that, when the peak ground acceleration (PGA) is small (0.1g), the structure response is almost in the linear stage, see Figs. 7(a) and 8(a), but when the PGA is larger (0.8g), strong nonlinearity occurs in both the constitutive curves and the restoring force curves (see Figs. 7(b) and 8(b)). The statistics of stochastic responses of the structure are shown in Fig. 9. Remarkably, different correlation configurations have only slight effects on the mean of the stochastic responses no matter the structure is in linear or nonlinear stage (see upper subplots in Fig. 9(a) and (b)), but have great effects on the standard deviation of the response (see lower subplots in Fig. 9(a) and (b)) according to whether the structure is in linear stage or not. When the structure is in linear or weakly nonlinear stage, the standard deviation of the responses changes little against different correlation configurations (Fig. 9(a)), whereas when the structure subjected to strong earthquake is in strong nonlinear stage, the standard deviation of response of structure with PD or CI configuration is much larger, by a factor of nearly 2, than that with CD configuration. This of course will affect the seismic reliability greatly. In particular, this demonstrates that the coupling of randomness and nonlinearity will lead to a great fluctuation in the structural responses [31].

4.3.2. Comparison between the probability densities and contours of stochastic responses for different correlation configurations

Noticing that the first two statistical moments are inadequate to represent the complete probabilistic information of the stochastic structural responses [13], the contours of PDF surface and typical PDFs of responses are shown in Figs. 10–11. From Fig. 10 , it is observed that the correlation configuration has significant influence in both linear and nonlinear cases.

The differences can also be easily identified from Fig. 11, where the coupling effect of randomness and nonlinearity is remarkable. Actually, in linear stage of the structure, the major shapes of PDF for the three correlation configurations are close to each other, as shown in Fig. 11(a), whereas in the strong nonlinear stage, the PDFs are quite different, see Fig. 11(b).

Remark 3. As noticed from Fig. 6 the majority part of points in CI and PD are similarly scattered, thus the statistic moments of the responses of CI and PD are close (see Fig. 9(b)). However, the points in the tail

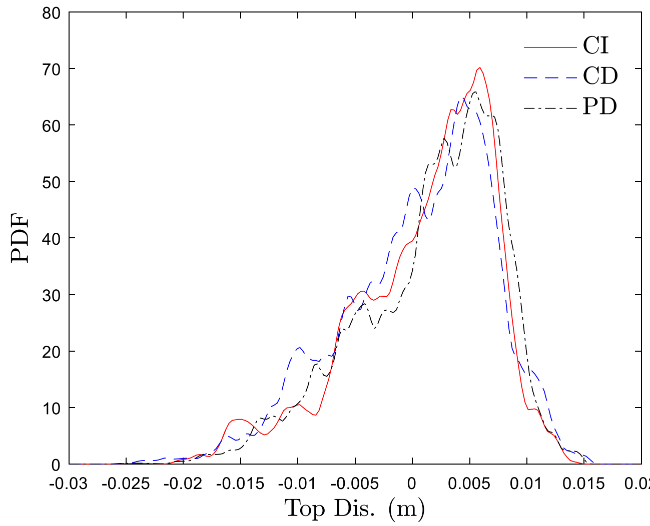

(a) Case 1: evolution PDFs are apparently different for three correlation configurations

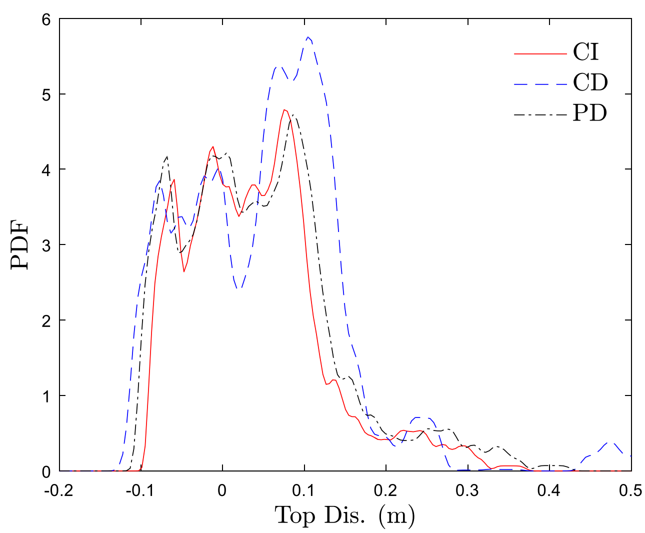

(b) Case 2: evolution PDF of CD is much different from the ones of CI and PD

Fig. 11. PDFs at specific time instant for three correlation configurations.

range are different, which leads to the detailed differences in the PDF curves (see Figs. 10 and 11).

4.4. Influence of correlation between inter-story parameters

Apart from the correlation between different mechanical parameters, there exists correlations between each story [32], which is not considered in the above analysis (see Table 1). In this section, we assume all the stories are completely dependent rather than independent, which means all mechanical parameters of concrete are identical from the 1st floor to the 10th floor. In this case, the model parameters are shown in Table 2 with details.

Table 2
Model parameters with randomness (all floors are identical/completely dependent).

Correlation	Parameters	Mean	Std.D	Distribution	Note
CI	f_c	30 MPa	6 MPa	Normal	–
	E_c	2.98×10^4 MPa	2.38×10^3 MPa	Normal	
CD	f_c	30 MPa	6 MPa	Normal	Eq. (16)
	E_c	–	–	–	
PD	f_c	30 MPa	6 MPa	Normal	Eq. (12)
	ζ	0	1	Normal	
	E_c	–	–	–	

The statistical moments of responses for the top and bottom displacements are shown in Fig. 12. Notice that when the structure is in linear stage, the correlation of each story has little influence (see Fig. 9(a) with Fig. 12(a)). However, when the structure is in strongly nonlinear stage, comparing Figs. 9(b) and 12(b) leads to the observations that: for the top displacement, the standard deviations of response in the case with completely dependency between each floor are higher by a factor nearly 2 than those in the case when the parameters of different floors are independent; however, for the bottom displacement, this property is totally opposite, i.e., the standard deviations of response in the case with completely dependency between each floor are even lower than those in the case when the parameters of different floors

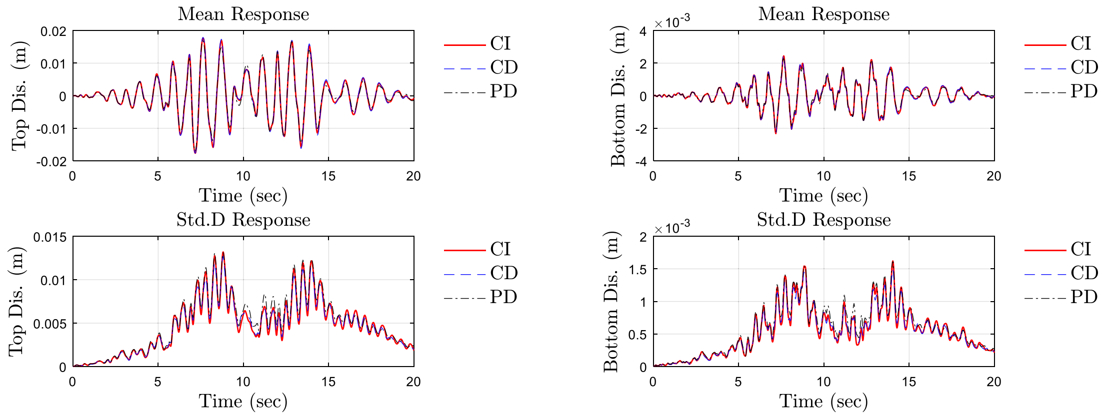

(a) Mean and Std.D of top and bottom displacement in case 1 (0.1g)

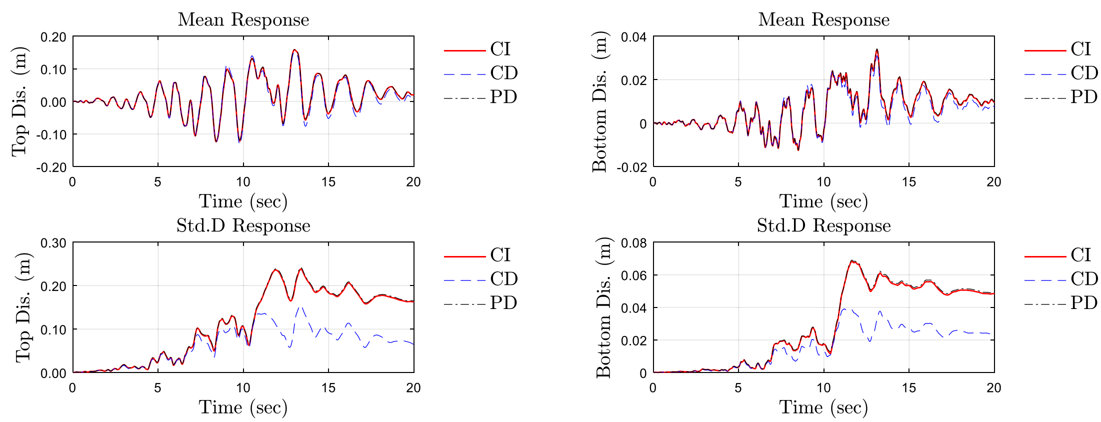

(b) Mean and Std.D of top and bottom displacement in case 2 (0.8g)

Fig. 12. Statistics of structural displacement responses (parameters of all floors are identical).

are independent. In fact, this performance is exactly due to the spatial variation of material properties [33], and more researches should be done in the future.

Clearly, what is more important is that, as the standard deviations of structural response are greatly affected by the correlation configuration in the strongly nonlinear stage, the reliability of the structure under strong earthquakes will thus be greatly different, and consequently should be carefully considered in structural design. Undoubtedly, more should be done in this aspect.

5. Concluding remarks

Practical mechanical properties of concrete structures are usually correlated, and may have unignorable effects on stochastic responses of structures. For this purpose, a physically-guided data-driven methodology of capturing correlation configuration of basic random variables and the probability density evolution method is synthesized in this paper to implement stochastic dynamic response of concrete structures with dependent random parameters. The main findings include:

(1) The physically-guided data-driven methodology can capture the correlation configuration of basic random variables by combining the physical mechanisms and observed data. Besides, possible physical constraints can be revealed.

(2) The point selection strategy based on the GF-discrepancy minimization should be adjusted based on the imposed physical constraints.

(3) The correlation configuration usually has only slight effects on the mean value of stochastic response in both linear and nonlinear situation, however, in the stage of strong nonlinearity, it has great effects by a factor of nearly 2 on the standard deviation of responses, and has remarkable influence on the PDF of stochastic responses. Besides, it is also remarkably noticed that, the correlation between the parameters of different floors has unignorable effects on the response, and for different response quantities, such effects are usually quite different, even qualitatively opposite. Consequently, the correlation configuration cannot be ignored in the decision-making of structural design under strong earthquakes.

Further studies, including the correlation configuration of random field parameters of structures and the response of structures involving randomness in both excitation and parameters, should be done in the future.

Acknowledgments

The supports of the National Natural Science Foundation of China (Grant Nos. 51725804, 11672209 and 51538010), the NSFC-DFG joint project (Grant No. 11761131014), the Committee of Science and Technology of Shanghai China (Grant No. 18160712800), and the Research

Fund for State Key Laboratories of Ministry of Science and Technology of China (Grant No. SLDRCE19-B-23) are highly appreciated.

References

[1] R.G. Ghanem, P.D. Spanos, Stochastic Finite Elements: A Spectral Approach, Springer, 1991.
[2] J. Li, Stochastic Structural Systems: Analysis and Modeling, Science Press, 1996 (in Chinese).
[3] G. Blatman, B. Sudret, An adaptive algorithm to build up sparse polynomial chaos expansions for stochastic finite element analysis, Probab. Eng. Mech. 25 (2010) 183–197.
[4] Ministry of Housing and Urban-Rural Development (MHURD) of the People's Republic of China, GB 50010-2010 Code for Design of Concrete Structures, China Architecture & Building Press, 2010 (in Chinese).
[5] A.H.-S. Ang, W. Tang, Probability Concepts in Engineering: Emphasis on Applications to Civil and Environmental Engineering, John Wiley & Sons, 2007.
[6] J.B. Chen, Z.Q. Wan, P.Y. Song, Random function model for dependent random variables, Sci. Sin.-Phys. Mech. Astron. 61 (1) (2018) 014609 (in Chinese).
[7] G.Q. Li, J.H. Li, Method of second moment matrix – on the reliability calculation of dependent stochastic vector, J. Chongqing Inst. Architech. Eng. 1 (1987) 55–67, (in Chinese).
[8] E. Torre, S. Marelli, P. Embrechts, et al., A general framework for data-driven uncertainty quantification under complex input dependencies using vine copulas, Probab. Eng. Mech. 55 (2019) 1–16.
[9] D.Q. Li, L. Zhang, X.S. Tang, et al., Bivariate distribution of shear strength parameters using copulas and its impact on geotechnical system reliability, Comput. Geotech. 68 (2015) 184–195.
[10] X.S. Tang, D.Q. Li, C.B. Zhou, et al., Copula-based approaches for evaluating slope reliability under incomplete probability information, Struct. Saf. 52 (2015) 90–99.
[11] M. Rosenblatt, Remarks on a multivariate transformation, Ann. Math. Stat. 23 (3) (1952) 470–472.
[12] C. Soize, R. Ghanem, Physical systems with random uncertainties: chaos representations with arbitrary probability measure, SIAM J. Sci. Comput. 26 (2) (2004) 395–410.
[13] L. Xu, G.D. Chen, Discussion on: moment methods for structural reliability, Struct. Saf. 25 (2003) 193–199.
[14] J. Li, J.B. Chen, Stochastic Dynamics of Structures, John Wiley & Sons, 2009.
[15] A. Papoulis, S.U. Pillai, Probability, Random Variables, and Stochastic Process, McGraw-Hill, 2001.
[16] J. Wei, An approach on the relation between elastic modulus and strength of concrete, J. Zhengzhou Univ. Eng. Sci. 3 (1987) 13–16 (in Chinese).
[17] L.X. Wu, J.H. Huo, A thoretical basis of equation of correlation between strength and elastic modulus of concrete, J. Chongqing Inst. Archit. Eng. 15 (1) (1993) 31–35 (in Chinese).
[18] China Academy of Building Research – Research Group on Basic Mechanical Properties of Concrete, Research Report on Reinforced Concrete – Some Basic Mechanical Properties of Concrete, China Architecture & Building Press, 1977 (in Chinese).
[19] J. Li, X.D. Ren, Stochastic damage model for concrete based on energy equivalent strain, Int. J. Solids Struct. 46 (2009) 2407–2419.
[20] J. Li, J.Y. Wu, J.B. Chen, Stochastic Damage Mechanics of Concrete Structures, Science Press, 2014 (in Chinese).
[21] J.B. Chen, J.Y. Yang, J. Li, A GF-discrepancy for point selection in stochastic seismic response analysis of structures with uncertain parameters, Struct. Saf. 59 (2016) 20–31.
[22] J. Li, Physical model for stochastic dynamic excitations of engineering structures, in: J. Li, J.B. Chen (Eds.), New Advances in Theory and Applications of Random Vibrations, Tongji University Press, 2009, pp. 119–132 (in Chinese).
[23] J. Li, Q. Yan, J.B. Chen, Stochastic modeling of engineering dynamic excitations for stochastic dynamics of structures, Probab. Eng. Mech. 27 (2012) 19–28.
[24] J. Li, J.B. Chen, The principle of preservation of probability and the generalized density evolution equation, Struct. Saf. 30 (2008) 65–77.
[25] J.B. Chen, R. Ghanem, J. Li, Partition of the probability-assigned space in probability density evolution analysis of nonlinear stochastic structures, Probab. Eng. Mech. 24 (2009) 27–42.
[26] J.B. Chen, J.P. Chan, Error estimate of point selection in uncertainty quantification of nonlinear structures involving multiple non-uniformly distributed parameters, Internat. J. Numer. Methods Engrg. 118 (2019) 536–560.
[27] D. Wang, J. Li, Physical random function model of ground motions for engineering purpose, Sci. China Tech. Sci. 54 (1) (2011) 175–182.
[28] Y.Q. Ding, Y.B. Peng, J. Li, A stochastic semi-physical model of seismic ground motions in time domain, J. Earthquake Tsunami 12 (3) (2018) 1850006.
[29] J.B. Chen, P.Y. Song, X.D. Ren, Stochastic dynamic response analysis of nonlinear structures with general nonuniform random parameters by minimum GL_2-discrepancy, Int. J. Multiscale Comput. Eng. 14 (3) (2016) 215–235.
[30] F.C. Filippou, E.P. Popov, V.V. Bertero, Effects of Bond Deterioration on Hysteretic Behavior of Reinforced Concrete Joints, Report EERC 83-19, 1983.
[31] J.B. Chen, J. Li, Stochastic seismic response analysis of structures exhibiting high nonlinearity, Comput. Struct. 88 (2010) 395–412.
[32] H. Zhou, J. Li, X.D. Ren, Multiscale stochastic structural analysis toward reliability assessment for large complex reinforce concrete structures, Int. J. Multiscale Comput. Eng. 14 (3) (2016) 303–321.
[33] J.B. Chen, J.R. He, X.D. Ren, J. Li, Stochastic harmonic function representation of random fields for material properties of structures, J. Eng. Mech. 144 (7) (2018) 04018049.